Polybasic Nanomatrices Prepared by UV-Initiated Photopolymerization

Omar Z. Fisher[†] and Nicholas A. Peppas*[,†,‡,§]

Departments of Biomedical Engineering, Chemical Engineering and Division of Pharmaceutics, University of Texas at Austin, 1 University Station C0400, Austin, Texas 78712-1062

Received August 29, 2008; Revised Manuscript Received March 27, 2009

ABSTRACT: A novel method for synthesizing nanoscale polymer networks that swell in acidic media is described here using photoinitiated emulsion polymerization. These nanomatrices consist of a cross-linked core of poly[2-(diethylamino)ethyl methacrylate] surface grafted with poly(ethylene glycol) (PDGP) with an average diameter of 50−150 nm. Control over mesh size, surface charge, encapsulation efficiency, and in vitro biocompatibility was obtained by varying cross-linking density. The ability to image nanomatrices in their dry state using conventional scanning electron microscopy was made possible by increasing cross-linking density. Theoretical calculations of matrix mesh sizes were supported by the encapsulation of both insulin and colloidal gold 2−5 nm in diameter. The ability to sequester and control the aggregation of an inorganic phase confirmed their use as a nanocomposite matrix material. These networks could be used as imaging agents, drug delivery devices, or components of sensing devices.

1. Introduction

Nanogels that exhibit aqueous swelling below a critical pH have many potential applications as nanoactuators, drug delivery devices, and sensing agents. Yet, they have received much lower attention than similar, self-assembled nanostructures. The advantage of cross-linking is enhanced structural integrity and control over swelling and transport properties. Here the emulsion polymerization of pH-responsive, polybasic nanoscale matrices using photopolymerization is described. The responsiveness is caused by the presence of weakly basic pendant groups that ionize at or below physiological pH. These networks can be tailored to encapsulate, deliver, or sequester specific therapeutic or diagnostic agents.

Gene delivery has been a widely investigated application for nanostructures based on weakly basic polyamines. Many of these polymers are amphiphilic and partially cationized at physiological pH. The presence of protonated amines along the polymer chain allows them to self-assemble into nanoparticulate polyelectrolyte complexes with polyanions, such as nucleotides. This electrostatic attraction can also be used to bind monoanions. For example, Renagel (sevelamer hydrochloride) and Renvela (sevelamer carbonate) are two clinically available polyamines that sequester phosphate ions for the treatment of chronic kidney disease. Likewise, these structures also bind to negatively charged groups on cell surfaces.[1,2] This explains their ability to gain entry into the cell, but it is also the reason for their significant toxicity.

The monomer 2-(diethylamino)ethyl methacrylate (DEAEM) is a tertiary amine containing methacrylate that can undergo free radical polymerizations. It has previously been used to synthesize homopolymers and various copolymers, in both its native and ammonium salt form. The resulting homopolymer, poly[2-(diethylamino)ethyl methacrylate] (PDEAEM), undergoes a pH-dependent phase change between hydrophobe and hydrophile.

PDEAEM precipitates out of aqueous solution at a pH above its pK_a and forms into a soft, tacky substance with a T_g below ambient temperature.[3] Shatkay and Michaeli[4] first described the buffering range of PDEAEM with respect to its pH-dependent phase transition. They determined that phase separation occurs at pH values just below the polymer pK_a. They observed a precipitation point at 7.48 and determined a pK_a of 7.68 by titration. Other groups have reported pK_a's between 7.0 and 7.3.[5] Siegel and Cornejo-Bravo[3,6] investigated the buffering properties of PDEAEM and its relationship to hydrophobicity. They showed that the polymer pK_a and water sorption decreases when DEAEM is copolymerized along with more hydrophobic monomers.

Schwarte and Peppas[7,8] used DEAEM in the fabrication of copolymer networks that display pH-triggered swelling. The mesh sizes of these networks could be controlled by varying comonomer feed and cross-linking ratios. These changes were verified by measuring the diffusion of large and small molecular weight solutes through the networks. These studies demonstrated the feasibility of PDEAEM networks as controlled drug delivery agents. However, the hydrophobicity of the networks above the critical swelling pH was compromised by introducing hydrophilic poly(ethylene glycol) (PEG) chains. Both Kost and Goldraich[9] and Hariharan and Peppas[10] used 2-hydroxyethyl methacrylate as a comonomer and attained similar results. Increasing the hydrophilicity of PDEAEM by copolymerizing with more hydrophilic monomers increases the network pK_a. These earlier studies were done using solution polymerization. A heterogeneous polymerization could take advantage of the hydrophobicity of DEAEM to obtain surface hydrophilicity while maintaining a separate, hydrophobic phase.

Another advantage of heterogeneous polymerization is that increased surface area can provide faster responsiveness. Podual and co-workers exploited the responsive properties of PEG grafted PDEAEM networks to make glucose responsive networks.[11−14] They showed that P(DEAEM-*g*-PEG) microgels, prepared in suspension, had a faster response to changes in pH than larger sized gels.[12] The size of PDEAEM-based networks was further reduced to the nanoscale using thermally initiated emulsion polymerization.[5,15,16] This method achieved nanomatrices from 50 to 700 nm that were charge and/or sterically stabilized in water. However, the synthesis required reaction times ≥24 h. A photoinitiated method could provide faster initiation and a much shorter reaction time.

* To whom correspondence should be addressed: e-mail peppas@che.utexas.edu, Tel 512 471 6644, Fax 512 471 8227.
[†] Department of Biomedical Engineering.
[‡] Department of Chemical Engineering.
[§] Division of Pharmaceutics.

10.1021/ma801966r CCC: $40.75
Published on Web 04/14/2009

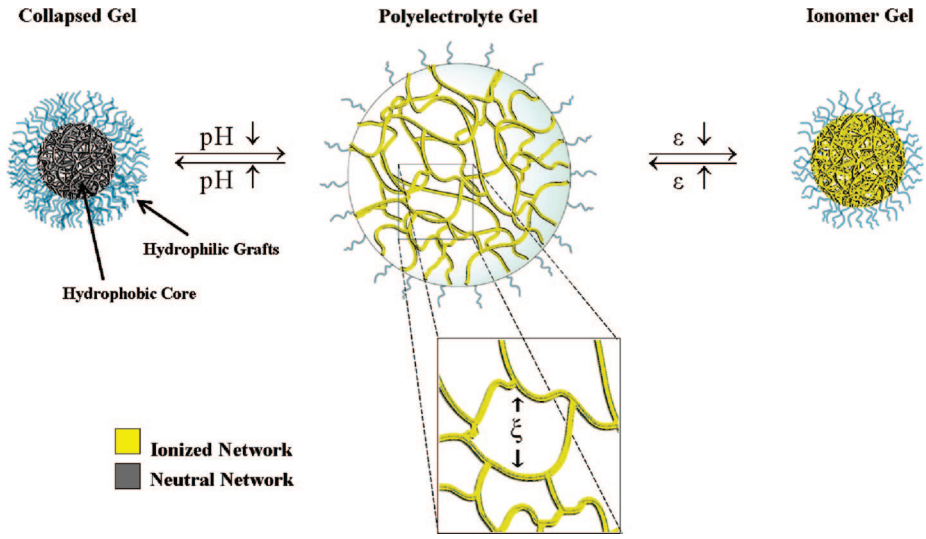

Figure 1. Environmental responsiveness: polybasic nanomatrices will ionize and swell in water at low pH. The influx of water increases the gel mesh size (ξ), allowing additional compounds to be loaded into the matrix. If the dielectric constant of the solvent (ε) is reduced, the gel will collapse into an ionomer.

Depending on the synthesis method, the buffering range of PDEAEM is either just above or slightly below the physiological pH of 7.4. A pK_a slightly below this would be ideal for most biomedical applications. For example, as an intracellular delivery agent a slight drop in pH would trigger the network to swell.[17−19] Copolymerizing DEAEM with more hydrophilic comonomers such as PEG increases the network pK_a by reducing the proton activity needed for ionization.[6] Emulsion polymerization can allow PEG to be surface grafted onto PDEAEM networks but not interfere with the buffering properties. The resulting system would also be water dispersible at all pH values.

The effect of cross-linking density on the nanoscale material properties of PDEAEM networks has not been fully determined. Because of the large surface area per mass of nanomatrices, they can swell to equilibrium much faster than larger systems. Enhanced cross-linking may not affect swelling as it would for larger systems. In this work the relationship between cross-linking density and network properties is investigated. Also, a novel synthesis strategy was developed to create pegylated PDEAEM nanomatrices more efficiently. The network morphology and cytocompatibility of these structures were studied to elucidate their potential as drug delivery agents.

2. Experimental Section

2.1. Materials. The chemicals 2-(diethylamino)ethyl methacrylate, Brij-30, Brij-35, bovine insulin, myristyltrimethylammonium bromide (MyTAB), poly(ethylene glycol) monomethyl ether monomethacrylate (M_n = 2080, 50 wt % aqueous solution) (PEGMMA), sodium dodecyl sulfate (SDS), tetrachloroauric(III) acid, tetraethylene glycol dimethacrylate (TEGDMA), and tetrakis(hydroxymethyl)phosphonium chloride (THPC) were all obtained from Sigma-Aldrich Corp. Deuterium chloride (DCl; 20% in D_2O), hydrochloric acid 1 N solution (HCl), Pluronic F-68, and sodium hydroxide 1 N solution (NaOH) were obtained from Thermo-Fisher Scientific. Irgacure 2959 was obtained from Ciba Chemical Co. Dulbecco's Modified Eagles Media (DMEM) and NIH/3T3 mouse fibroblasts were obtained from American type Culture Collection (ATCC, Manassas, VA). Bovine calf serum and 10× phosphate buffered saline (PBS) were obtained from Mediatech Inc. Deuterium oxide (D_2O) was obtained from Cambridge Isotope Laboratories Inc. (Andover, MA).

2.2. Photoemulsion Polymerization. PDGP nanomatrices were polymerized by emulsion polymerization as described: All monomers were passed through a column of basic alumina powder to remove inhibitor prior to use. In a glass beaker, a mixture TEGDMA and DEAEM was added to a 50 mL aqueous solution of 5 wt % PEGMMA, Irgacure 2959 at 0.5 wt % of total monomer, and various surfactants in deionized distilled water (ddH_2O). A range of surfactant mixtures were evaluated to determine which was best suited for maintaining emulsion stability and which would achieve the smallest nanogel size. Emulsion stability was checked by placing a drop of the emulsion between a glass slide and coverslip and viewing it at 40× objective magnification. If the coalescence of fat droplets could be viewed, then the emulsion was deemed unstable. TEGDMA was used at X values of 0.01, 0.025, 0.05, 0.10, and 0.20, where X is the cross-linking mole feed ratio. The DEAEM content was kept constant at 5 wt % monomer in water.

The mixture was emulsified for 10 min using a Misonix Ultrasonicator (Misonix Inc., Farmingdale, NY) at 88 W while partially submerged in a stirred ice water bath. The emulsion was then purged with nitrogen gas for 10 min, capped, and then exposed to a UV point source for 2 h at 140 mW/cm^2 with the light guide directed at the top of the emulsion, all with constant stirring. PDEAEM homopolymer and cross-linked networks were prepared using the same synthesis conditions without PEGMMA and TEGDMA or just without PEGMMA. PDGP graft copolymer was prepared using the same conditions but without cross-linking.

The removal of unreacted reagents and surfactants was performed by collapsing, aggregating, and centrifuging the suspended particles in their cationized state. First, an equal volume 1 N HCl was added to the suspension to fully protonate the particles. Acetone was then added to the suspension up to a final concentration of 70%, the point at which the particles flocculated and began to sediment. The mixture was then centrifuged at 3200g for 10 min to fully separate out the precipitate. The solvent was then poured off, and the pellet was resuspended again in 0.5 N HCl. The precipitation/centrifugation/resuspension steps were repeated five times with a final resuspension in water. The suspensions were then dialyzed (MWCO = 15 kDa) for 5 days, with water being replaced twice daily, until the pH of the supernatant matched the pH of water. The suspension was then flash frozen in liquid nitrogen, lyophilized, and finally placed in a vacuum oven at 30 °C until further use. Polymers prepared without cross-linker were precipitated similarly but centrifuged at 33000g.

3. Results and Discussion

3.1. Photoemulsion Polymerization. A successful emulsion polymerization scheme for the synthesis of PEG surface-grafted poly[2-(diethylamino)ethyl methacrylate] (PDGP) nanomatrices was determined empirically and qualitatively. The goal was to

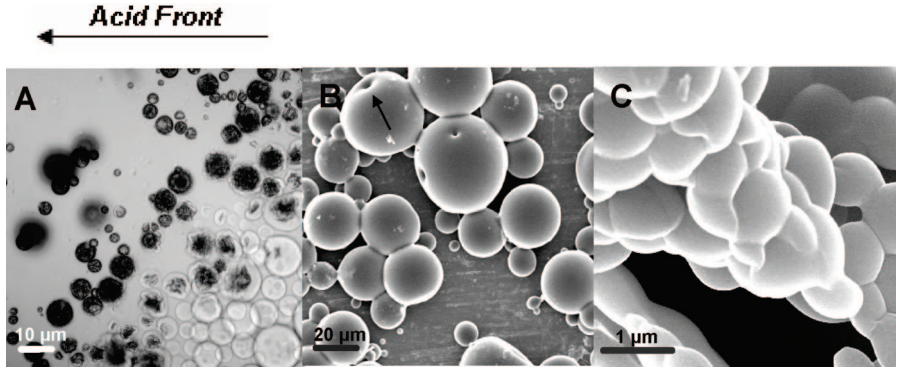

Figure 2. PDGP microgels. (A) Light microscope image of a microgel suspension, prepared using Pluronic F-68, swelling in an approaching hydrochloric acid front. (B) SEM image of dried PDGP microgels prepared with Pluronic F-68. (B) Microgels prepared from a Pluronic F-68 emulsion. Arrow points to pores that were observed on the surface of larger particles. (C) SEM image of microgels prepared using SDS.

attain nanomatrices that behaved as shown in Figure 1, where a transition between collapsed gel, polyelectrolyte gel, and ionomer gel is shown. These states were exploited for processing and loading.

In oil-in-water emulsion polymerization the self-assembly of surfactants into micelles is required. Although a two-phase system is established, polymerization begins not in the water or monomer droplet phase but in the micellar phase. For this reason the concentration of surfactants used must be above the critical micellar concentration (cmc). Growing nanoparticles are continuously fed monomer and free radicals from the surrounding water phase. The rate of polymerization can be increased by reducing the size of the monomer droplets.[20]

In this work monomer droplet size was checked using optical microscopy. Droplet size was influenced by mechanical agitation as well as choice and concentration of surfactant. When initially compared, ultrasonication for 10 min resulted in smaller droplet sizes than ultrahomogenization at 24 000 rpm. The size distribution also appeared to be narrower when ultrasonication was used. Sonication was used for all further investigations. The emulsion was established using ultrasonication and maintained throughout the polymerization by mechanical stirring. This is in contrast to other schemes where mechanical stirring is used both to create and maintain the emulsion throughout the reaction. This required that the emulsion remain stable after sonication.

The ionic surfactants, myristyltrimethylammonium bromide (MyTAB) and sodium dodecyl sulfate (SDS), were able to both establish and maintain macro- and microemulsions at concentrations ranging from 0.5 to 3 times the critical micellar concentration (cmc). However, microemulsions did not produce detectable particles. SDS was used first, as a proof of concept, because of its success in previous work.[5] The cationic surfactant MyTAB was chosen as a replacement to eliminate the possibility of electrostatic attraction between the surfactant and the particles during the surfactant removal process. When used alone, none of the nonionic surfactants were able to sustain microemulsions at any concentration. When Pluronic F-68 at 0.2−2 wt % was used, the result was acid swellable microgels with diameters in the 0.8−50 μm range. These contained large internal cavities that were only visible when the gels were swollen (Figure 2A). These could have been the result of incomplete suspension polymerization or a pseudo-w/o/w emulsion. The evacuation of these large cavities under vacuum may have resulted in the pores seen using scanning electron microscopy (Figure 2B). The use of Brij-35 and Triton X-100 achieved similar results. Using SDS below the cmc achieved microgels 0.8−1 μm in diameter (Figure 2C).

A mixture of 3.4 mM MyTAB with any nonionic cosurfactants was successful in maintaining emulsion stability. However, MyTAB with 2 mg/mL Brij-30 was the only surfactant mixture that resulted in particle diameters well below 1 μm. The polydispersity and average particle size were also dependent on the concentration of Brij-30. Both of these were lowered when the concentration of Brij-30 was increased to 4 mg/mL. Using Brij-30 alone was unable to maintain emulsion stability. Brij-30 is distinct from the other nonionic surfactants used because of its low hydrophile−lipophile balance ratio (HLB). A nonionic surfactant with an HLB ratio of $\geq$10 is typically used for an oil-in-water emulsion. Those with an HLB ratio of $<$10 are typically used for inverse emulsions. The HLB ratio for Brij-30 is 9.7. The HLB ratios for Triton X-100, Pluronic F-68, and Brij-35 are 13.5, 24, and 16.9, respectively, as provided by the manufacturers.

According to previous work, a minimum PEG graft size of 2 kDa is needed to minimize nonspecific protein adsorption.[21] The use of molecular weights that were higher than 5000 was shown to be less efficient. This is likely due to their tendency to form tighter coils. In this work a length of 2000 was chosen for preliminary work. Amalvy and coworkers[5] were able to use methacrylated PEG grafts alone, as both steric stabilizer and emulsifier, in the thermoinitiated emulsion polymerization of nanomatrices. The use of poly(ethylene glycol) monomethyl ether monomethacrylate (PEGMMA) (MW = 2080) alone in our work was insufficient in maintaining emulsion stability yet when removed from the reaction, there was visible flocculation after reacting for 1 h. To confirm that PEGMMA was acting as a steric stabilizer, it was replaced with PEG monomethyl ether (MW = 1900) in one reaction. This suspension also flocculated and settled to the bottom of the flask after 1 h. Polymer networks could be obtained in as little as 15 min. But a reaction time of at least 2 h was needed to obtain nanomatrices that did not flocculate in water above a pH of 7.3. This provided an observable way to check for the presence of PEG grafts on the surface. These observations were later confirmed by NMR.

The removal of surfactant and unreacted monomer from nanomatrices was achieved by inducing a polyelectrolyte-to-ionomer transition.[22] The chloride salt form of the tertiary amine is present when PDGP is suspended in water containing sufficient hydrochloric acid. The network can be collapsed while keeping the pendant groups ionized by lowering the dielectric constant of the suspension (Figure 1). This could be done by adding a weak organic solvent. When 70% acetone was added to nanomatrices suspended in 0.5 N hydrochloric acid (HCl), the transition from swollen gel to collapsed ionomer was achieved. This caused immediate flocculation and sedimentation of the particles. The ionomer phase was then isolated by centrifugation. The pellet could then be resuspended in water, and the process was repeated. The unreacted monomers and

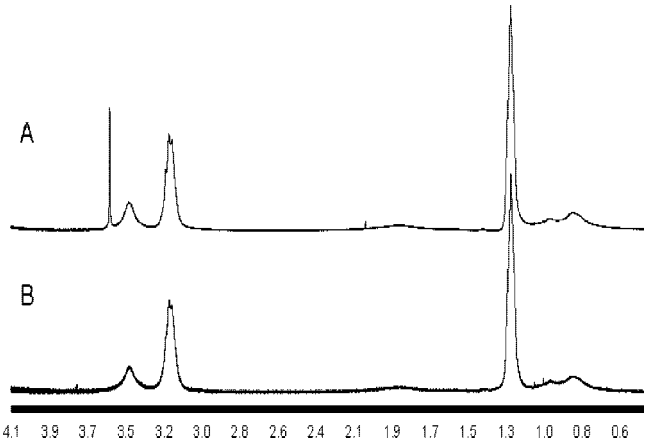

Figure 3. Proton NMR spectra of un-cross-linked PDGP (a) and PDEAEM (b).

surfactants were checked and found to be all soluble in 70% acetone in 0.5 N HCl. After a final resuspension in water, the excess hydrochloric acid could be washed out by dialysis. Un-cross-linked PDEAEM and PDGP would precipitate into a suspension that could be separated from the solvent, but only by using a much higher centrifugal force than for networks.

3.2. ^{1}H NMR Analysis. The ^{1}H NMR spectra for PDGP showed the additional presence of the oxyethylene peak from PEG grafts when compared to the spectra for PDEAEM, confirming pegylation (Figure 3). The absence of the oxyethylene peak in the PDEAEM sample also confirmed the removal of Brij-30. The amount of comonomer incorporated onto the network was quantified by comparing the ratio of peak area for the methylamine peak at 3.2 ppm to that of the oxyethylene peak area at 3.6 ppm. Specifically

$$^1\text{H ratio} = \frac{A_{\text{PEG}} - A_{\text{B,PEG}}}{A_{\text{meth}} - A_{\text{B,meth}}} \quad (1)$$

where A_{PEG} is the peak area of the oxyethylene group, $A_{\text{B,PEG}}$ is the area of background with the same ppm spread, A_{meth} is the peak area for the methylamine, and $A_{\text{B,meth}}$ is the area of background with the same ppm spread as the methylamine. The comonomer ratio could be calculated from the proton ratio by using the number of protons on each pendant group. For PDGP the DEAEM/PEGMMA ratio was 226, or 4.7 wt % PEG. The spectrum for the pegylated compound matches that published by Amalvy and co-workers[5] for a lightly cross-linked microgel. When NMR spectra were measured for cross-linked particles, signal attenuation was significant and increased with the cross-linking feed. Also, as the cross-linking feed increased, the oxyethylene peak area increased while all other peak areas decreased, relative to the background. While this effect confirms that the PEG is confined to the surface, analysis of the spectra would result in an overestimate of pegylation.

The practical advantage of keeping the particles in their fully protonated state after processing was that they were more easily handled than deprotonated samples. Deprotonated, dried nanomatrices were soft and tacky. This is consistent with the film-forming property of PDEAEM containing micro- and nanomatrices observed in other work.[5] This property also presents a complication for electron microscopy. Because PDGP particles tend to spread on a surface at ambient temperature, it was virtually impossible to observe their morphology using conventional scanning electron microscopy. The same is true for unfixed biological soft tissue. The common solution is to use a cross-linking agent such as gluteraldehyde to enhance the integrity of the sample. We attempted to determine whether increased cross-linking had a similar effect of the nanomatrices.

Scanning electron microscopy showed that the ability to discern the size and morphology of nanomatrices was dependent upon ionization and cross-linking density. In general, the ionized salt form of the PDGP networks gave the particles greater integrity under the electron beam. Large, ionized microparticles with 1 mol % feed cross-linking prepared from a Pluronic F-68 emulsion appeared spherical but typically had pores resulting from the rapid escape of encapsulated solvent (Figure 2B). Replacing Pluronic with SDS resulted in smaller, flattened spheres that tended to dry as monolayers (Figure 2C). Nanomatrices synthesized from a MyTAB/Brij-30 emulsion, with 1 mol % cross-linker in the feed, tended to form semicoherent films with the vague outline of particles visible in some places (Figure 4A). Cross-linking at 2.5% achieved a similar result. At 5−20% cross-linking the spherical shape of fairly monodisperse protonated nanoparticles became clear (Figure 4B,C). For 10% and 20% cross-linked nanomatrices the shape was preserved in both the protonated and deprotonated state.

3.3. Mesh Size. Dynamic light scattering measurements were used to determine the volume of nanomatrices in the swollen state (see Supporting Information for methods). The accuracy of the technique depended on size distribution. The use of Brij-30 below an aqueous concentration of 4 mg/mL resulted in a bimodal distribution of particle sizes. The polydispersity for batches made below this limit was between 0.25 and 0.4. Also, contrary to expectations, the measured hydrodynamic diameter of these batches decreased as a function of pH (i.e., they responded as if they were polyacidic networks). This was resolved by centrifuging the suspension at 40000*g* and thereby separating out the larger particles. This resulted in a suspension with polydispersity consistently <0.100 and the predicted swelling characteristics of a polybasic network. Increasing the Brij-30 concentration during synthesis achieved the same results. The ability to image nanomatrices at higher cross-linking feed values using electron microscopy was crucial in calculating the

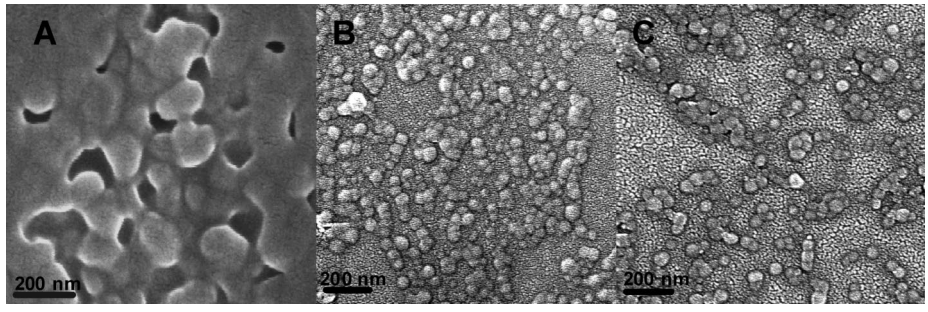

Figure 4. PDGP nanomatrices. (A) Protonated nanomatrices prepared from a MyTAB/Brij-30 emulsion, with 1 mol % cross-linker. (B) Deprotonated nanomatrices prepared from a MyTAB/Brij-30 emulsion, with 5 mol % cross-linker. (C) Protonated nanomatrices prepared from a MyTAB/Brij-30 emulsion with 5 mol % cross-linker.

volume swelling ratio Q. This value is defined as the ratio of network volume in the swollen state to the volume in the collapsed state. Assuming that each particle formed in the emulsion is a discrete bulk polymerization, the Brannon−Peppas model for polybasic networks with non-Gaussian chain length distributions can be used to determine the molecular weight between cross-links, $\overline{M}_c$.[7,23,24]

$$\frac{V_1}{4I}(\bar{v}Q)^{-2}\left(\frac{K_b}{10^{pH-14}+K_b}\right)^2 = \left[\ln\left(1-\frac{1}{Q}\right)+\frac{1}{Q}+\chi q^{-2}\right]+\frac{\left(\frac{V_1}{\bar{v}\overline{M}_c}\right)\left(1-\frac{2\overline{M}_c}{\overline{M}_n}\right)\left(Q^{-1/3}-\frac{Q}{2}\right)\left(1+\frac{1}{N}Q^{-1/3}\right)^2}{\left(1-\frac{1}{N}Q^{-2/3}\right)^3} \quad (2)$$

Here V_1 is the molar volume of water (18 cm^3/mol), I is the ionic strength of the swelling medium, calculated as 1.7 for phosphate buffered saline (PBS), and $\bar{v}$ is the specific volume of the polymer, 0.91 g/cm^3. K_b is the basic dissociation constant for DEAEM, χ is the Flory polymer−solvent interaction parameter, previously estimated as 0.20,[10] and $\overline{M}_n$ is the molecular weight of the un-cross-linked polymer, equal to a value of 14.9 kDa as obtained by gel permeation chromatography (GPC) measurements. N is the number of consecutive units between cross-links, calculated as

$$N = \frac{\frac{M_n}{M_r}}{\frac{M_n X}{M_r}+1} \quad (3)$$

Values of the molecular weight between cross-links and mesh sizes in swollen state are listed for each formulation in Table 1. These experimental values were used to compute a network mesh size. This value is a physical distance between cross-links and can be used to estimate the upper size limit of agents that can diffuse into and out of the matrix. Assuming an isotropic extension of polymer chains upon swelling, the mesh size can be modeled as

$$\xi = Q^{1/3}\left[C_n\frac{2\overline{M}_c}{M_r}\right]^{1/2} l \quad (4)$$

where C_n is the characteristic ratio for a methacrylate network ($C_n = 11$) and l is the carbon−carbon bond length (0.154 nm). The volume of particles in the dry state was calculated as the cube of the average particle diameter from SEM images. The diameter was measured by drawing lines across a minimum of 30 particles in images taken at each cross-linking feed ratio and scaling them relative to the scale bar. A single average diameter of 50 ± 10 nm was used for all calculations of Q since the measured diameters for cross-linking feed ratios of 0.5, 0.10, and 0.20 were not significantly different.

The estimate for N is based on an idealized, equal distribution of chain junctions, where the un-cross-linked chain is divided into $n+1$ equally spaced segments and n is equal to the degree of polymerization multiplied by the cross-linking feed ratio (eq 2). This estimate is not required when using the model for Gaussian chain length distributions, which is applicable for very lightly cross-linked hydrogels.[23] When the mesh sizes obtained using either the model for Gaussian or non-Gaussian chain length distributions were compared, the values did not vary much for higher cross-linking values, though they did generally increase when using the Gaussian assumption. For samples with cross-linking feed ratios of 1%, 2.5%, 5%, and 10% the mesh size increased by 5.44, 0.77, 0.37, and 0.3 nm, respectively, relative to calculations based the assumption of a non-Gaussian chain length distribution was used. The reason for this trend is the relatively small value of M_n and the large influence of cross-linking. Using an artificial value of 1000 kDa for M_n increased the mesh size for the 1% cross-linked formulation by 5 nm but had negligible impact on samples cross-linked at 2.5%, 5%, and 10%. The degree of swelling and mesh sizes for the formulations are plotted as a function of pH in Figure 5. No detectable swelling was measured for samples cross-linked at 20%. The network mesh sizes that were determined reach a maximum just below physiological pH.

Previous attempts to measure volume swelling for submicron particles have relied solely on light scattering data for spatial measurements.[5] When initial analyses were performed using light scattering measurements at high pH as geometric minimums, the estimated $\overline{M}_c$ and ξ values were unrealistic. Using

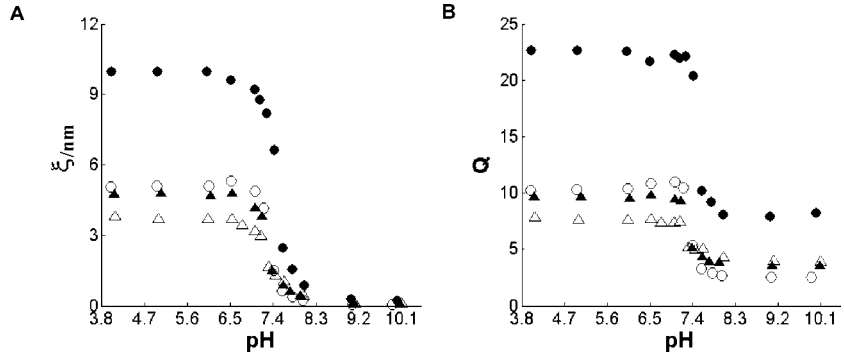

Figure 5. Mesh size (A) and volume swelling ratio (B) measurements as a function of pH for formulations with cross-linking ratios of 0.01 (●), 0.025 (○), 0.05 (▲), and 0.10 (△).

Table 1. Critical Swelling pH (pH_{cr}), Hydrodynamic Diameter (D_H) and ζ-Potential in the Swollen and Collapsed State, and Molecular Weights between Cross-Links (M_c) and Mesh Sizes (ξ) in the Swollen State for Different Cross-Linking Mole Feed Ratios (X)

		D_H (nm)		ζ (mV)			
X	pH_{cr}	pH = 6	pH = 8	pH = 6	pH = 8	M_c	ξ (nm)
0.01	7.60	141 ± 2	99 ± 1	32 ± 4	4.7 ± 3	4414	9.90
0.025	7.59	111 ± 2	68 ± 1	25 ± 5	−1 ± 4	1915	5.04
0.05	7.38	107 ± 1	76 ± 1	20 ± 6	−1 ± 6	1766	4.74
0.10	7.31	99 ± 1	78 ± 1	14 ± 2	−1 ± 2	1302	3.80

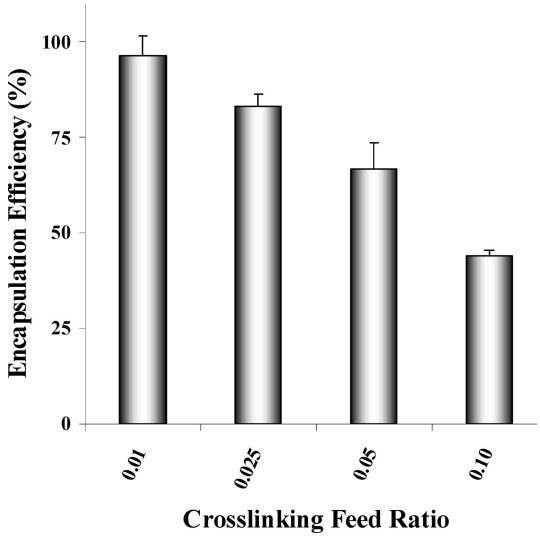

Figure 6. Insulin entrapment efficiency into PDGP nanomatrices at pH 7.4 for different cross-linking densities. Error bars = standard deviation ($n = 3$).

these values predicted that a particle with a cross-linking feed ratio of 0.025 had a larger degree of swelling than one less cross-linked. These also predicted a maximum mesh size of less than 1.5 nm. This precludes the entrapment of even relatively small macromolecules such as insulin, which has a monomeric radius of 1.3 nm.[25]

The diameters obtained from light scattering were expected to be slightly higher than in the dry state due to the presence of the surface grafted PEG chains. These were expected to increase the diameter by up to 7 nm based on the Flory radius for a PEG tether with a molecular weight of 2 kDa.[26] Yet, the formulation with the lowest cross-linking density had a volume ~220% of what would be expected. Despite the hydrophobic nature of the particle core, the larger increase can be accounted for by water absorption. Cornejo-Bravo and Siegel[3] investigated the ability of deprotonated, dry PDEAEM to absorb water from the vapor phase. It was determined that this absorption occurred in the form of nucleation around the pendant amines. While not enough to solubilize the polymer, this process did double the dry weight and had a plasticizing effect. Many insoluble natural fibers such as cellulose are plasticized by water in the same way.[27]

3.4. Insulin Loading. To confirm the ability to macromolecule loading into the network, we used insulin as model drug. Loading studies were done over a pH range of 6.5−7.4 (see Supporting Information for methods). HPLC measurements of the nanomatrix supernatant taken at a pH of 6.5 showed that 100% of insulin was uptaken at the two lowest cross-linking densities, 92 ± 0.3% for a molar feed ratio of 0.05 and 63 ± 0.7% for a molar feed ratio of 0.10. For all except nanomatrices with a molar feed ratio of 0.01, the values decreased as the pH was raised to 7.4 (Figure 6). Because the loading was performed at a pH above the pI for insulin, the protein was effectively a polyanion, which allowed it to form a polyelectrolyte complex with the polycationic polymer, in the same manner as polyplex formation. This additional electrostatic attraction may make the nanomatrices potentially useful in gene delivery. A network would be more stable than other self-assembled carriers such as lipopolyplexes, which are prone to degradation in serum.[28] The results showed that the networks could load up to their own weight in a model macromolecule and that loading decreased with decreasing mesh size. The drop in loading as the pH was raised likely resulted from the desorption of surface bound insulin. The loss of charge attraction caused the release of this insulin back into solution.

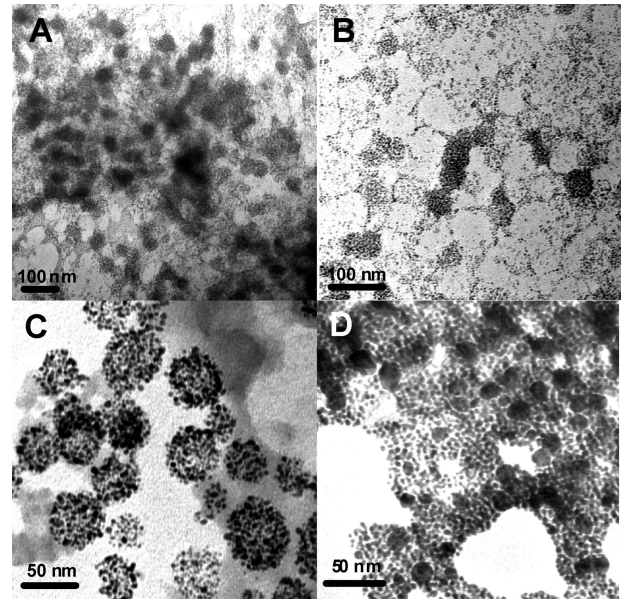

Figure 7. Transmission electron micrographs of colloidal Au loaded into PDGP nanomatrices with cross-linking feed ratios of 0.01 (A), 0.025 (B), 0.05 (C), and 0.10 (D).

3.5. Colloidal Gold Loading. Recently, there has been significant interest in the design of micro- and nanoscale composite inorganic/organic systems. The goal is to combine the advantages of macromolecular chemistry with the unique optical and electrical properties of inorganic nanosystems. For example, colloidal gold, 5−20 nm in diameter, can be trapped into thermoresponsive hydrogel microspheres, making them environmentally responsive imaging agents.[29] Though much of the research on hydrogels in this area has been limited to microgels,[30] there has also been work to synthesize submicron polymer nanocomposites.[31] Inorganic nanoparticles, such as gold colloids, can be as small as 1 nm in diameter. PDGP nanomatrices theoretically have a network structure that can accommodate particles of this size by simple partitioning. Gold colloids are also known to associate with basic amines, such as the pendant groups on PDGP networks, due to electrostatic attraction.[32−35] They also aggregate at pH extremes, resulting in a red shift in their extinction spectrum. Au colloids, 2−5 nm in diameter, do not have a distinct characteristic plasmon absorption peak in the visible light range.[36] But the controlled flocculation of these particles causes the appearance of a peak at 520 nm, typical of particles 5−30 nm in diameter. When loaded into PDGP nanomatrices, the network constraints on growth should cause the aggregation of gold nanoparticles to be mesh size limited. To test this, we loaded colloidal gold, 2−5 nm in diameter, into the nanomatrices and lowered the pH to induce aggregation (see Supporting Information for methods). The amount of acid added was based on the amount needed to cause a visible color change, from orange-black to blue, in the metal colloid alone. All the samples appeared to support the controlled growth of colloids up to particles 5 nm in diameter (Figure 7). This was confirmed by the presence of an extinction peak at 510 nm for the three lowest cross-linking values and a peak at 520 nm for the highest. The extinction spectra for 1−5% cross-linked samples were identical. But there was noticeable spectral broadening for the sample with the 10% cross-linking density, suggesting the presence of gold nanoparticles larger than 5 nm (Figure 8). Suspensions of nanomatrices alone had no discernible absorbance peak at any wavelength, at the concentrations used.

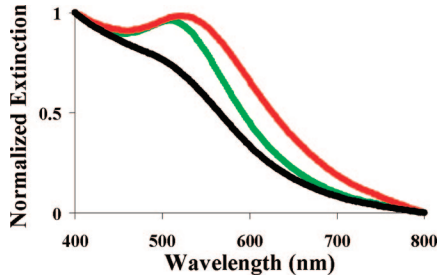

Figure 8. Extinction spectra for Au loaded nanomatrices with 5% (green) and 10% (red) cross-linking and Au colloid alone (black).

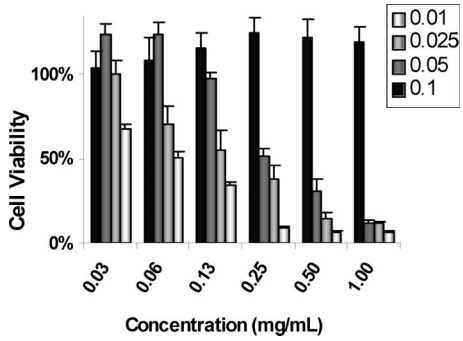

Figure 9. MTS assay of NIH/3T3 fibroblasts exposed to PDGP nanomatrices as a function of concentration and cross-linking density. Each bar represents the mean ± standard deviation ($n = 8$).

Transmission electron microscope (TEM) images showed the presence of 2−5 nm gold particles for samples with a cross-linking feed ratio of 0.01 and 0.025 concentrated within flattened, spread particles in a semicoherent film (Figure 7A,B). This matched the film forming seen with SEM. At 5% cross-linking all the gold colloid was localized within polymer particles, with diameters between 30 and 70 nm (Figure 7C). Nanogels cross-linked at 10% accommodated gold nanoparticles up to ~5 nm within the polymer networks, but there was also the presence of larger gold particles 10−25 nm associated around the particles (Figure 7D). This suggested that the gold colloid was partly confined to the outside of the nanomatrices, where it was free to form larger aggregates. The polymer networks also appeared to aggregate around the larger gold aggregates. The mesh size calculations predicted that at 10% cross-linking density the network would support little aggregation. This theory fits with the visible exclusion of larger gold particles to the surface of the polymer particle shown in the figure. Confined to the surface, the gold aggregation should eventually overcome the presence of PEG grafts and cause the networks to flocculate.

3.6. Cell Viability. The biocompatibility of PDEAEM-based micro- and nanostructures depends on how cationized the pendant amine groups are at physiological pH and how exposed they are to the biological environment. The use of PEG as a steric stabilizer has been shown to increase the in vitro biocompatibility of PDEAEM nanogels,[15] yet it is still far below that of similar nanogels[37] or polyplexes.[38] PDGP nanogels show a distinct positive relationship between cross-linking density and cytocompatibility (Figure 9). The IC_{50} values for nanogels with 1%, 2.5%, and 5% cross-linker monomer feed were 62.5, 125, and 250 μg/mL, respectively. Samples made with 10% cross-linker monomer feed caused no reduction in cell viability at any concentration tested (see Supporting Information for methods).

Anderson and Mallapragada[39] investigated the in vitro cytocompatibility of linear chains of PDEAEM copolymerized with PEG and determined a nontoxic concentration up to 3 μg/mL using NIH/3T3's. Oishi and co-workers[15] also observed a positive relationship between cross-linking density and cytocompatibility for PDEAEM nanogels up 1% cross-linked, but the authors only compared two different cross-linking ratios. It was postulated that more cross-linking inhibits the free dangling of cationic chain segments, thereby reducing their ability to interact with cell membranes. This is reasonable, given the soft and rubbery nature of the polymer.

The results of this work showed that a change in the buffering range of the system also occurs with increased cross-linking by making the core of the particle more hydrophobic. Siegel and Cornejo-Bravo[6] demonstrated this effect on linear PDEAEM by copolymerizing with a more hydrophobic comonomer. An increase in the proton energy needed to swell the system would translate into less cationization at a given pH, as predicted by the Henderson−Hasselbalch model.[40] This could also lead to a more biocompatible system.

4. Conclusions

We have successfully used photopolymerization to synthesize polybasic nanogels capable of encapsulating therapeutic agents that can also serve as scaffolds nanocomposite fabrication. The advantage of using photoinitiation as a driving force was that we achieved a significantly more time efficient reaction than similar emulsion-based methods for making PDEAEM-based nanogels.[5,15,16] The PEG-stabilized nanogels displayed pH-dependent volume swelling with a hydrodynamic diameter between 50 and 150 nm. By varying cross-linking density, we could control the network mesh size and thereby limit the loading of both insulin and gold colloids. This also had the effect of increasing the in vitro biocompatibility of the networks. These have the potential to be used as templates for the controlled growth of other micro- and nanostructures, components of sensing and diagnostic devices, or carriers for the targeted delivery of therapeutic agents.

Acknowledgment. N.A.P. acknowledges support from the National Institutes of Health, Grant EG-000246, and from a National Science Foundation Integrative Graduate Education and Research Traineeship (IGERT) Fellowship (to O.Z.F.), DGE-03-33080. The authors also acknowledge the technical assistance of Helen Lin in the Department of Biomedical Engineering, the resources of the University of Texas at Austin Institute for Cellular and Molecular Biology, and the Texas Material Institute.

Supporting Information Available: Experimental methods used for GPC, NMR, SEM, TEM, dynamic and electrophoretic light scattering, insulin and colloidal gold loading, and cell viability measurements.This material is available free of charge via the Internet at http://pubs.acs.org.

References and Notes

(1) Labat-Moleur, F.; Steffan, A. M.; Brisson, C.; Perron, H.; Feugeas, O.; Furstenberger, P.; Oberling, F.; Brambilla, E.; Behr, J. P. *Gene Ther.* **1996**, *3*, 1010.
(2) Behr, J. P. *Chimia* **1997**, *51*, 34.
(3) Cornejo-Bravo, J. M.; Siegel, R. A. *Biomaterials* **1996**, *17*, 1187.
(4) Shatkay, A.; Michaeli, I. *J. Phys. Chem.* **1966**, *70*, 3777.
(5) Amalvy, J. I.; Wanless, E. J.; Li, Y.; Michailidou, V.; Armes, S. P.; Duccini, Y. *Langmuir* **2004**, *20*, 8992.
(6) Siegel, R. A.; Cornejo-Bravo, J. M. *ACS Symp. Ser.* **1992**, *480*, 131.
(7) Schwarte, L. M.; Peppas, N. A. *Polymer* **1998**, *39*, 6057.
(8) Schwarte, L. M.; Peppas, N. A. *Abstr. Pap. Am. Chem. Soc.* **1997**, *214*, 292.
(9) Kost, J.; Goldraich, M. *Abstr. Pap. Am. Chem. Soc.* **1992**, *203*, 113.
(10) Hariharan, D.; Peppas, N. A. *Polymer* **1996**, *37*, 149.
(11) Podual, K.; Doyle, F.; Peppas, N. A. *Ind. Eng. Chem. Res.* **2004**, *43*, 7500.
(12) Podual, K.; Doyle, F. J.; Peppas, N. A. *Biomaterials* **2000**, *21*, 1439.

(13) Podual, K.; Doyle, F. J.; Peppas, N. A. *J. Controlled Release* **2000**, *67*, 9.
(14) Podual, K.; Peppas, N. A. *Polym. Int.* **2005**, *54*, 581–593.
(15) Oishi, M.; Hayashi, H.; Itaka, K.; Kataoka, K.; Nagasaki, Y. *Colloid Polym. Sci.* **2007**, *285*, 1055.
(16) Hayashi, H.; Iijima, M.; Kataoka, K.; Nagasaki, Y. *Macromolecules* **2004**, *37*, 5389.
(17) Boussif, O.; Lezoualch, F.; Zanta, M. A.; Mergny, M. D.; Scherman, D.; Demeneix, B.; Behr, J. P. *Proc. Natl. Acad. Sci. U.S.A.* **1995**, *92*, 7297.
(18) Akinc, A.; Thomas, M.; Klibanov, A. M.; Langer, R. *J. Gene Med.* **2005**, *7*, 657.
(19) Sonawane, N. D.; Szoka, F. C.; Verkman, A. S. *J. Biol. Chem.* **2003**, *278*, 44826.
(20) Piirma, I. *Emulsion Polymerization*; Academic Press: New York, 1982.
(21) Moghimi, S. M.; Hunter, A. C.; Murray, J. C. *Pharmacol. Rev.* **2001**, *53*, 283.
(22) Osada, Y., Khokhlov, A. R., Eds. *Polymer Gels and Networks*; Marcel Dekker: New York, 2002.
(23) Brannon-Peppas, L.; Harland, R. S. *Absorbent Polymer Technology*; Elsevier Science Pub.: New York, 1990.
(24) Brannon-Peppas, L.; Peppas, N. A. *Chem. Eng. Sci.* **1991**, *46*, 715.
(25) Oliva, A.; Farina, J.; Llabres, M. *J. Chromatogr., B: Biomed. Sci. Appl.* **2000**, *749*, 25.
(26) Wong, J. Y.; Kuhl, T. L.; Israelachvili, J. N.; Mullah, N.; Zalipsky, S. *Science* **1997**, *275*, 820.
(27) Espert, A.; Vilaplana, F.; Karlsson, S. *Composites, Part A* **2004**, *35*, 1267.
(28) Li, S.; Tseng, W. C.; Stolz, D. B.; Wu, S. P.; Watkins, S. C.; Huang, L. *Gene Ther.* **1999**, *6*, 585.
(29) Kuang, M.; Wang, D. Y.; Mohwald, H. *Adv. Funct. Mater.* **2005**, *15*, 1611.
(30) Pich, A. Z.; Adler, H. J. P. *Polym. Int.* **2007**, *56*, 291.
(31) Owens, D. E.; Eby, J. K.; Jian, Y.; Peppas, N. A. *J. Biomed. Mater. Res. A* **2007**, *83A*, 692.
(32) Oldenburg, S. J.; Averitt, R. D.; Westcott, S. L.; Halas, N. J. *Chem. Phys. Lett.* **1998**, *288*, 243.
(33) Westcott, S. L.; Oldenburg, S. J.; Lee, T. R.; Halas, N. J. *Langmuir* **1998**, *14*, 5396.
(34) Averitt, R. D.; Westcott, S. L.; Halas, N. J. *J. Opt. Soc. Am. B* **1999**, *16*, 1824.
(35) Nehl, C. L.; Grady, N. K.; Goodrich, G. P.; Tam, F.; Halas, N. J.; Hafner, J. H. *Nano Lett.* **2004**, *4*, 2355.
(36) Duff, D. G.; Baiker, A.; Edwards, P. P. *Langmuir* **1993**, *9*, 2301.
(37) McAllister, K.; Sazani, P.; Adam, M.; Cho, M. J.; Rubinstein, M.; Samulski, R. J.; DeSimone, J. M. *J. Am. Chem. Soc.* **2002**, *124*, 15198.
(38) Funhoff, A. M.; van Nostrum, C. F.; Koning, G. A.; Schuurmans-Nieuwenbroek, N. M.; Crommelin, D. J.; Hennink, W. E. *Biomacromolecules* **2004**, *5*, 32.
(39) Anderson, B. C.; Mallapragada, S. K. *Biomaterials* **2002**, *23*, 4345.
(40) Hasselbalch, K. A. *Biochem. Z.* **1916**, *78*, 112.

MA801966R